ARTICLE

Targeted removal of blood cancer cells from mixed cell populations by cell recognition with matching particle imprints

Received 00th January 20xx,
Accepted 00th January 20xx

DOI: 10.1039/x0xx00000x

Perrine Remaud,[a] Jevan Medlock[a], Anupam A. K. Das[a], David J. Allsup[b], Leigh A. Madden[c], Dieter Nees,[d] Paul J. Weldrick[a] and Vesselin N. Paunov[a]*

We report a new approach for separation of blood cancer cells from healthy white blood cells based on cell recognition by surface functionalised particle imprints. We prepared polymeric particle imprints from a layer of suspension of monodisperse PMMA microbeads which closely match the size of in-vitro cultured human leukaemia cells (HL60). The imprints were replicated on a large scale with UV curable polyurethane resin using Nanoimprinting lithography and surface functionalized with a cationic polymer, branched polyethylene imine (bPEI) and a Pluronic surfactant, Poloxamer 407, to exert a weak attraction towards the cells. The latter is amplified several orders of magnitude when a cell of closely matching size and shape fits into the imprint cavity which multiplies the contact area between cell surface and the imprint cavity. The particle imprints were optimised for their specificity toward the blood cancer cells by treatment with oxygen plasma and then subsequent coatings with bPEI and Poloxamer 407 with various functionalisation concentrations. We tested the surface functionalised imprints for their specificity in retaining in vitro cultured human leukaemic cells (HL60) over healthy human peripheral blood mononuclear cells (PBMCs) in a flow through chamber. The effect of the flushing flow rate of over the mixed cell solution suspension over the particle imprint and the particle imprint length were also investigated. At each step the selectivity towards HL60 was assessed. Selective isolation of an increased amount of HL60 tumour cells over PBMC was ultimately achieved as a function of cell seeding ratio on the particle imprint. The effect is attributed to the substantial size difference between the HL60 cell and the PBMCs. The data presented show that relatively inexpensive PMMA microbeads imprints can be utilised as a cell separation technique which could ultimately lead to novel therapies for removal of the neoplastic cells from peripheral blood of acute myeloid leukaemia patients.

Introduction

Bioimprints are polymeric replicas of cells or microorganisms which produce surface cavities of the same shape and size as the original cells.[1,2] These polymer based cavities then can be optimised to allow specific recognition of the target cells of matching size and shape. The bioimprint acts in the same principle as that of the Lock and Key model which enables the shape and size based recognition of specific cells.[1,3-5] The first report of bioimprints is credited to Dickert *et al*.[6] who created a highly selective yeast imprint from a sol-gel matrix. Further whole cell imprints have been made from a range of micro-organisms and human cells. As utilised here, Hayden *et al*.[7] functionalised red blood cell polyurethane imprints capable of distinguishing cells via blood group antigen recognition. Subsequently they were able to separate cells from blood groups A1 and A2.[8] Molecular imprinted polymers have also been utilised for biological applications such as bacteria, virus and chemical sensing. [9-11] The advantages of imprinting technologies lie in their ease of manufacture, stability, reusability and importantly, specificity for biological targets. [12]

Acute myeloid leukaemia (AML) presents as uncontrolled proliferation of neoplastic cells (myeloblasts) causing an imbalance in haematopoiesis leading to bone marrow failure and resulting in a death of the patient if untreated.[13-15] In the UK, the average overall 5-year survival is 16% from the point of diagnosis. The prognosis is significantly worse in the majority of patients due to disease presentation in the later years of life.[13,16-19] Current AML treatment is myeloablative chemotherapy followed by an allogeneic stem cell transplant.[20-21] AML patients spend a long time hospitalised and suffer considerable morbidity related to anaemia, sepsis and bleeding. Outcomes for AML patients have only improved in relation to supportive care pathways rather than any new drug regimens.[22] There is an urgent need to seek alternative therapies for these patients. Selective leukophoresis can potentially be used more in the extraction of myeloblasts from peripheral blood which is critical in stabilizing AML patients with leukostasis associated with hyperleuocytosis.[23] By reducing the number of circulating tumour cells, the likelihood of early relapse is also diminished.[24]

[a] Department of Chemistry and Biochemistry, University of Hull, Hull, HU67RX, UK.
[b] Hull York Medical School, University of Hull, University of Hull, Hull, HU67RX, UK.
[c] Department of Biomedical Sciences, University of Hull, Hull, HU67RX, UK.
[d] Joenneum Research FmbH, Leonhardstrasse 59, 8010 Graz, Austria.
*Corresponding author: V.N.Paunov@hull.ac.uk, Tel: +44 1482 465660.
♣Electronic Supplementary Information (ESI) available: See DOI: 10.1039/x0xx00000x

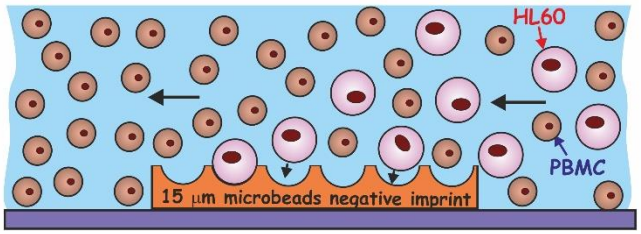

Figure 1. The principle of particle imprint-based AML cell depletion from a mixture with PBMCs. The substantially larger (AML) cells are preferentially attracted and retained on the imprint due to large contact area whereas smaller, healthy PBMCs are flushed through with little interaction.

AML blood cancer cells present an ideal target for cell shape recognition by prefabricated bioimprinted surfaces where a very strong specific adhesion can occur between the imprinted cell surface pattern and the cells of matching shape. The separation between the myeloblasts and healthy white blood cells on a particle imprint should occur due to the distinct cell size and morphological differences between the myeloblasts and normal blood cells (Figure 1). The cell surfaces are normally negatively charged due to the presence of integral proteins and carbohydrates with negatively charged COO^- groups on the phospholipid bilayer.[25] Hence, the imprints can be first treated with a biocompatible cationic polyelectrolyte to promote attractive electrostatic interaction between the target cells and the imprint surface. The polymeric imprints can be potentially used for various applications in different fields due to their low production cost, unique mechanical, thermal and chemical properties, their stability and their ease to be prepared.[26] The molecular imprinting technology has been used in many different areas such as separation methods, biosensors, organic synthesis and drug development.[27] This imprinting technology also has great prospects in the field of biomedicine hence, this study is aimed at the development of matching imprints for medical applications such as a supplementary therapy for blood cancer that can be used alongside conventional chemotherapy. There are two types of methods to create imprinted polymers[28] the cell-membrane-molecular imprinting and the whole-cell-imprinting strategy. The former use only a part of the cell surface while the second method replicates the cells as a whole entities or constituent bio-macromolecules. We have recently utilised a bioimprinting approach to remove tumour cells from healthy cells.[29] This approach, whilst successful would be time consuming to replicate for individual patients where a bioimprint must be made from the individuals tumour cells, which would first have to be isolated from whole blood. A simple particle imprint of matching target cell size could simplify this approach and negate the requirement for individualised bioimprints. However, casting cells with polymers opens a range of challenges as the cells can potentially shrink, flatten and change their shape during the replication process due to drying or upon contact with the resins. In this project, a novel imprinting strategy using monodisperse poly(methylmethacrylate) (PMMA) microbeads of a similar size to target blood cancer cells (~14 μm) was used to mimic the whole cell bioimprinting. The strategy is reminiscent of the method used to fabricate micro-lenses arrays by dual templating of monodisperse particle monolayers with PDMS and UV-curable optical adhesive.[40] Its application produced a positive imprint a microbeads layer imprint which could then be upscaled using the Roll-to Roll-nanolithography method (R2R NIL).[30] In order to increase the selectivity of the particle imprint towards the blood cancer cells the particle imprint was first treated with the cationic polyelectrolyte bPEI in order to promote attractive electrostatic interaction between the target cells and the particle imprint surface. In order to weaken the attraction and make the interaction cell-imprint more specific with respect to the cell shape and size, a secondary treatment in the form of POL407 was used to passivate the surface of the positively charged particle imprint in order to make healthy white blood cells less likely to non-specifically attach to the imprint. Hence the interaction needs to be weak enough to rely on the amplification of the contact area between the cells and the imprint cavities surface. The function of the POL407 is to offset the approaching cells from imprint which weakens the attraction. This is needed to reduce the non-specific adhesion of the PBMCs with the imprint upon point contact, while magnifying the interaction between HL60 cells and the imprint cavities. The particle imprint used for this specific study was made using 15 μm PMMA microbeads (Spheromers™ CA15, Microbeads) (Fig. 2) which have matching size to the targeted HL60 cells of average diameter of 14 μm (See Figure S1, ESI).

Materials and Methods

Preparation of CA15 particle imprints

Spheromers® C15 microbeads were sourced from Microbeads AS, Norway (www.micro-beads.com). Glass substrates (70 cm × 40 cm) were cleaned with acetone and alcoholic KOH (10 wt%) for 1 h, washed with deionized water and treated with 20 wt% poly(diallyldimethylammonium chloride) (PDAC) aqueous solution for 30 min, followed by further cleaning with deionized water drying under air stream. A sample of 6.0 g of Spheromers® CA15 PMMA microbeads, 2.5 g of glucose was mixed together in 30 mL of 0.1% (w/v) % xanthan gum solution. Spreading of this CA15 suspension on the glass substrate was done using a glass tool comprised of a square frame of four glass strips, one of which was offset by 100 μm to create a gap. The CA15 suspension was added to the frame cavity and the tool was moved over the glass substrate (with a lead) in a steady motion in the direction opposite to the higher side. This allowed an aqueous film of CA15 microbeads suspension (40 cm × 70 cm) of uniform thickness (~100 μm) to be deposited, followed by evaporation to a semi-dry state at room temperature in a laminar flow cabinet. Curable Sylgard 184 elastomer (polydymetylsiloxane, PDMS, from Dow Corning) was mixed at a 10:1 ratio of elastomer to accelerator and degassed by 10 min centrifugation at 4000g. A metal frame of interior space 65×30×4 cm was placed on top of the produced CA15 microbeads layer and the PDMS elastomer solution (900 mL) was poured evenly inside.

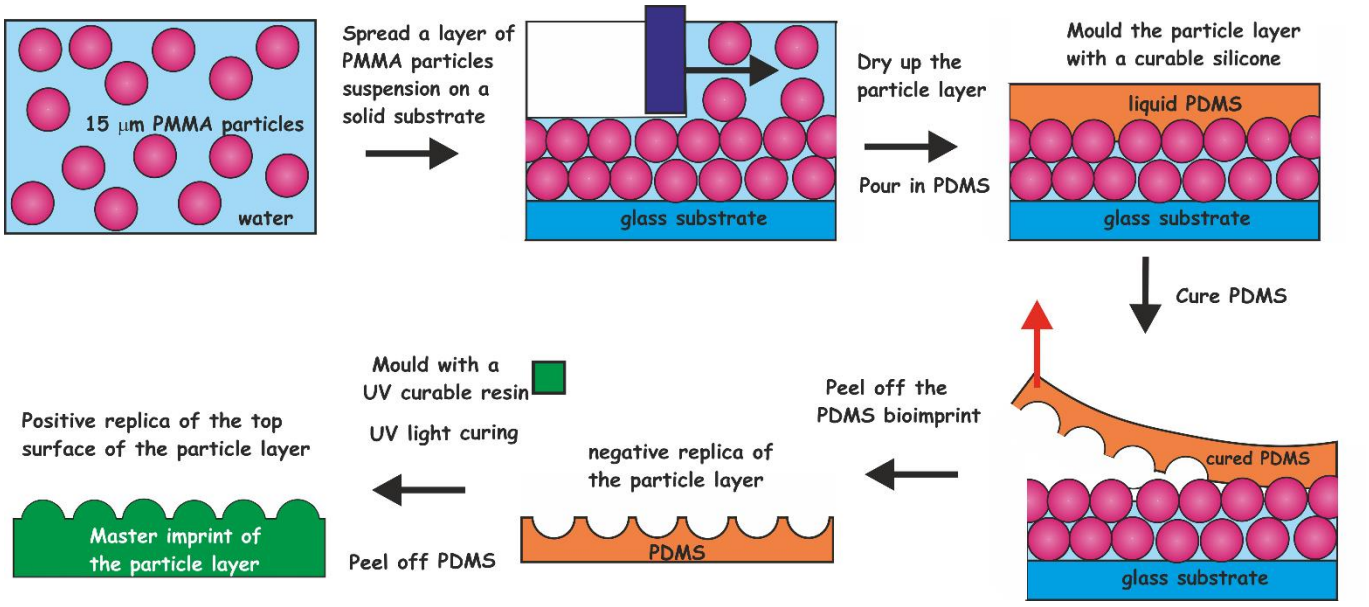

Figure 2. The process of imprint production from PMMA microbeads layers. CA15 PMMA particles were formulated as an aqueous suspension containing glucose and spread evenly over a glass substrate. The produced microbeads layer was levelled off with a bespoke tool and dried up in air. The microbeads layer was casted with curable silicone (PDMS). The latter was peeled off after 24 h of curing and cleaned up to make a negative imprint. This imprint was casted a second time with UV-curable polyurethane (PU) resin and to produce a positive imprint (shim) which was used in replication of the original patter by Roll-to-Roll Nanoimprinting (see Figure S2, ESI).

For structural support, a polyester fabric sheet (Boyes UK, dimensions 65×30×0.1 cm) was added on top of the PDMS layer and the composite was allowed to cure at 25 °C for 48 h. The cured PDMS cast of the CA15 microbeads layer was peeled off the glass surface and washed using warm aqueous solutions of detergent, ethanol and deionized water in sequence, followed by drying under air stream. The negative PDMS imprint (Figure 3A,B) was then replicated further onto a polyethylene terephthalate (PET) foil with a pre-deposited layer of photo-curable PU-acrylic resin (supplied from Joanneum Research FmbH, Graz, Austria).

Surface modification of CA15 particle imprints

The negative CA15 microbeads imprints on PET foil were cut in different lengths (2, 4, 8 and 12 cm) x 8 mm and were further surface functionalised to incur a weak attraction between target HL60 cells and the imprint. The particle imprint samples were first treated with oxygen plasma (Harrick Plasma PDC 32G) at 147 Pa, using an RF power of 16 W for 4 min. The oxygen plasma treated CA15 imprint samples were further incubated for 15 minutes with aqueous solutions of the cationic polyelectrolyte branched polyethylene imine (bPEI, Polysciences Inc) with different concentrations (0.01%, 0.015%, 0.02%, 0.025%, 0.03%, 1% and 2% (w/w)). Further, they were rinsed with deionised water and air-dried before being integrated in the PDMS-based flow-through chip (Figure 4A,B) in order to test the CA15 microbeads imprint selectivity towards HL60 cells in a mixture with PBMCs and HL60 cells. Additional treatment of the imprint and the whole chamber and tubing with solutions of Poloxamer 407 (Sigma Aldrich) was applied, with a range of POL407 concentrations of 0.25%, 0.5%, 1%, 2% or 3% (w/w) in deionised water which were loaded in the PDMS-based chip after the bPEI-treated particle imprint was integrated in the chip. The imprint was incubated with the POL407 solution for 30 min and finally washed by flushing with 10 mL of Phosphate Buffered Saline (PBS, Corning) at a flowrate of 219 mL/hr using a syringe pump (World Precision Instruments SP100i Syringe Pump). Tapping mode atomic force microscopy was carried out using a Dimension Edge (Bruker) with TESPA-V2 probes (Bruker). A scan rate of 0.1 Hz was used with 1024 or 512 lines for a 50 μm scan range (Figure 3C-3D).

Flow-through imprint device

A Phosphate Buffer solution at 5 mM was prepared by adding 0.78 g of sodium dihydrogen orthophosphate dihydrate (Fisher Chemicals) in 1 L of deionised water. The pH was adjusted to 3 using orthophosphoric acid (Fisher Chemicals). The solution was heated at 50°C and 1 g of hydroxypropyl methylcellulose (HPMC) (sourced from Dow Chemical Company) was added slowly to the solution in order to obtain a solution of hydroxyl HPMC at 0.1% (w/v). Sylgard 184 elastomer (10:1 elastomer: accelerator, Dow Corning) was mixed thoroughly and degassed by centrifugation (Sorvall Biofuge Primo, Thermofisher Scientific) at 5000 g for 10 min. 3 mL of the HPMC solution was put in glass substrates and was incubated for 30 min.

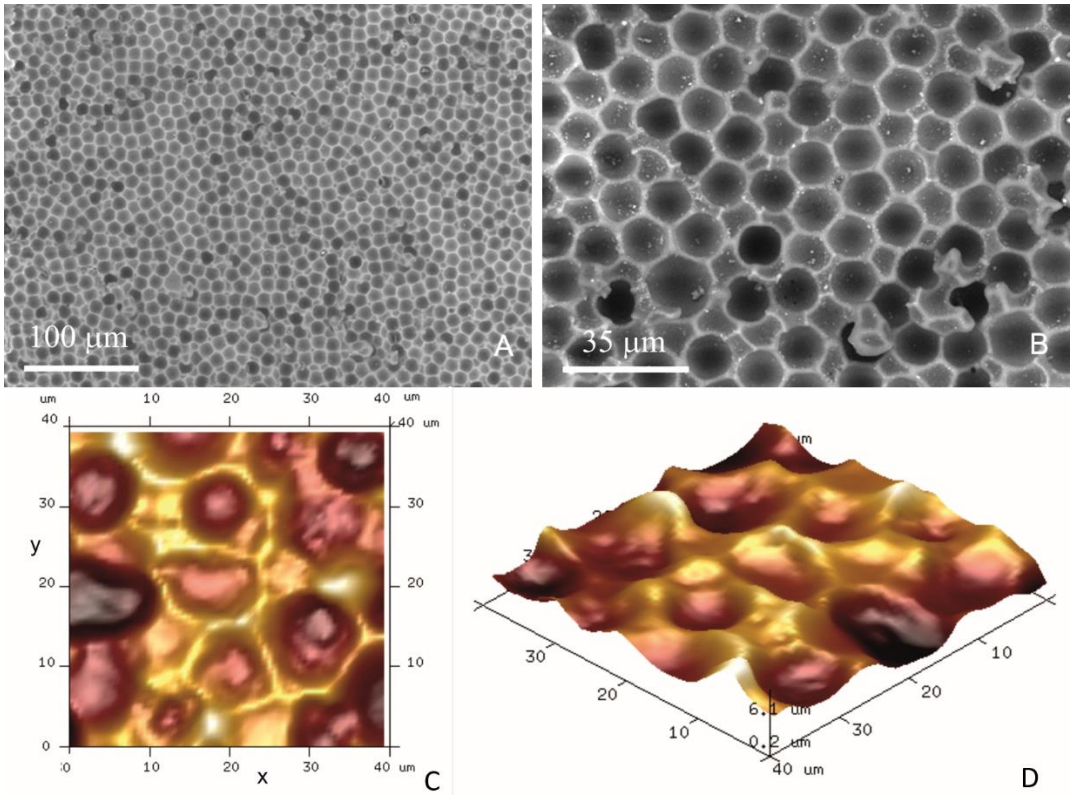

Figure 3 SEM images of typical negative PDMS imprints of a layer of 15 µm PMMA microbeads (Spheromers® CA15) deposited on a glass slides as suspension. The scale bars represent (A) 100 µm and (B) 35 µm, respectively. (C-D) Atomic force microscope images of the CA15 particle imprints with different perspectives.

It was rinsed with water and air dried. 25 mL of PDMS-hardener 10:1 mixture was poured over glass substrates (5×50×1mm) with the microbeads layer, immobilised on the glass surface, and left to cure at 40°C for 24 h. The PDMS was removed from the glass surface in order to yield identical channels on PDMS substrates. The microscope slide (ThermoScientific) and PDMS channel was treated with Oxygen Plasma (1100 mTorr, 32 W) for 2 min. The prepared microbeads imprint was placed over the channel aperture and the glass slide used to enclose the system (Figure 4). The device was clamped together and in a drying oven at 40°C for 30 min. Inlets and outlets were added by puncturing the PDMS and feeding with PTFE tubing (~ 0.5 mm diameter).

Cell retention tests, staining and counting

HL60 cells (sourced from Public Health England) were cultured aseptically in a mixture of 80 mL of Roswell Park Memorial Institute Medium (RPMI) 1640 (Gibco), mixed with 10 mL foetal bovine serum (Gibco), 5 mL penicillin and 5 mL streptomycin solutions (Lonza) at 37°C with 5% CO_2. PBMCs were obtained from anonymous apparently healthy donors via the NHS blood transfusion service (under IRAS 214660 with REC ethical approval 16/LO/1948) and stored in liquid nitrogen prior to use. PBMCs are composed of monocyte and lymphocyte populations and the shape and size are generally accepted to be the same to a large degree, flow cytometry can highlight the cell populations without the need for additional staining to differentiate between monocytes and lymphocytes. The cells were slowly defrosted and washed 3 times in PBS. Removal of platelet contamination was achieved by triple centrifugation at 120g for 10 min and resuspension in PBS. HL60 cells surfaces were fluorescently tagged by dropwise addition of 100 µL of 0.025 wt% 1,2-dioleoyl-sn-glycero-3-phosphoethanolamine N(carboxy-fluorescein) in ethanol to 2 mL of the stock HL60 cell suspension (1×10^6 cells/mL). PBMCs were treated via a similar method using 1,2-dioleoyl-sn-glycero-3-phosphoethanolamine-N (Lissamine rhodamine B sulphonyl) (ammonium salt). The cells were washed twice separately using centrifugation (VWR, Mega Star 3.0R) at 400g for 5 min. The supernatant was removed and the cells were redispersed in deionised water. The cells were counted using an Improved Neubauer haemocytometer observed under the microscope. An Olympus BX51 fluorescence microscope coupled with a mercury lamp excitation source and DP70 camera (Olympus) with ImageProPlus software was used to acquire images of the captured cell populations retained on the CA15 imprint.

Mixed cell sample preparation

The desired amount of cells was taken from the master stock suspensions of PBMC and HL60 cells and transferred into two tubes (Eppendorf) in order to have a (HL60/PBMC) cell ratio of 25%/75% or 10%/90%, respectively measured by number of cells.

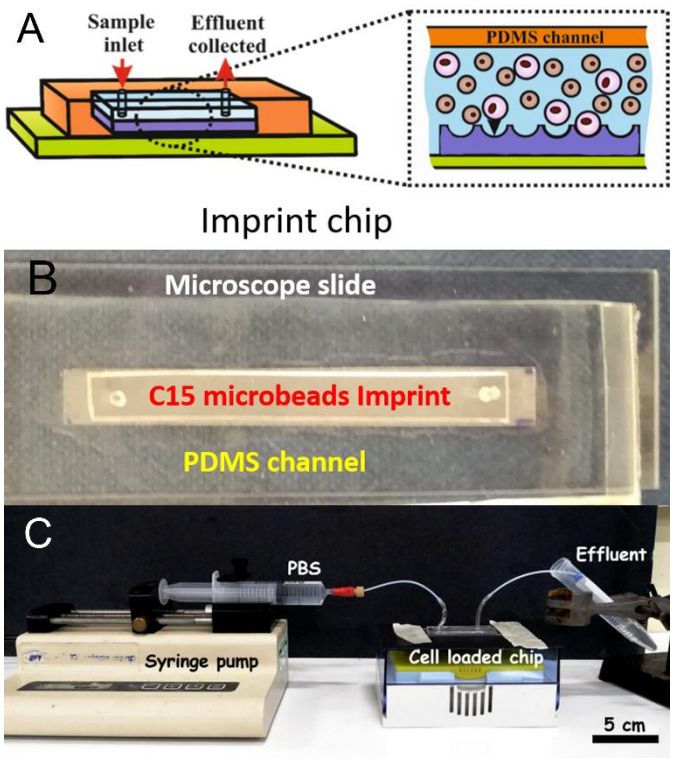

Figure 4 (A) Schematic and (B) top side view of the actual particle imprint (of length 4 cm and width 6 mm) attached on a microscope slide with PDMS channelled casing with input and output channels. Scale bar is 1 cm. (C) Photographs showing the setup used for the static experiment using the syringe pump the cell loaded chip and the collected effluent.

The ratios were chosen to mimic *in vivo* blast loads in AML where diagnosis is made at a blast proportion of 20%.[31] The same ratio of (HL60/PBMC) cells was loaded into the fluidic chips of different imprint lengths. The total number of cells was calculated to be enough in order to saturate the smallest imprint (6.54×10^5 cells for the 2 cm chip, 1.31×10^6 cells for the 4 cm chip). PBS buffer was used to top up the total volume of the cell suspension to 1 mL. The suspensions were centrifuged at 400g for 6 min (with Minispin Plus Eppendorf centrifuge). The supernatant was then removed leaving the separated cells in the tube. PBS buffer was added to the PBMC tube (2 cm: 50 µL, 4 cm: 100 µL, 8 cm: 200 µL and 12 cm: 300 µL), mixed with the cells and then with the HL60 cell suspension at the desired ratios (see below). The centrifuge tubes were sonicated using an ultrasonic bath for 5 min to prevent any cell aggregation. The prepared mixed cell suspension of the desired cell ratio was injected into the fluidic imprint chip and allowed to be settle on the imprint for 30 min. 10 mL of PBS was eluted over the particle imprint at different flowrates (50 mL/hr, 126 mL/hr or 219 mL/hr) using a syringe pump (see Figure 4C). The CA15 particle imprint samples with the residual cells were analysed by bright field and fluorescence microscopy by taking images before and after flushing of the chip. The HL60 and PBMC cells on the imprint were counted using the ImageJ software using the macro script described in ESI. In the case of multiple seeding of the imprint with the HL60/PBMC cell mixture, the cells solution was added to the chip after the flushing step with PBS without removing the retained cells from the previous run. Cell viability was not determined throughout the tests as the latter are time consuming and it is very challenging to keep every batch of cells with the same viability. It was not possible to test viability by this method as the cells were already fixed stained for recognition purposes with dyes that would be detected with the same fluorescence emission. However, in principle it could be tested using an Annexin V staining procedure prior to flow cytometry analysis. Retention of HL60 cells was assessed by taking images (n=10) with bright field and fluorescence microscopy at various sites across the bioimprint. Cells were enumerated via the automatic method using images collected using FITC and TRITC in order to separately assess each cell type collected at each site. Each experiments was reproduced upto 3 times and the standard deviation calculated from these results.

Results and Discussion

The EDX results presented in Figure S8 (ESI) clearly show that there is nitrogen present on the surface of the CA15 negative particle imprints after the treatment with 0.015 wt% bPEI and 0.03 wt% bPEI. In comparison, the non-treated CA15 particle imprint sample showed has no nitrogen. Note that the nitrogen content on the surface increases with the increase of the bPEI concentration. We characterised the average diameter of the CA15 imprint cavities which were determined to be 12.9 ± 0.9 µm (Figure S3 and Table S1, ESI). Note that this value does not correspond to the equatorial diameter of the templated CA15 particles which is 14.5 ± 0.4 µm. The reason being that the glucose layer filled the voids of the CA15 layer and obstructed the replicating resin to avoid formation of "necks" in the imprinted particles which would make impossible for a cell of the same radius of curvature to freely fit in. The average diameters of the HL60 cells and the PBMCs are 13.1 µm and 9.2 µm, respectively. This substantial difference between the radii of curvature of the malignant and the health white blood cells and the close match of the former to the CA15 microbeads imprint makes possible to selectively retain them on the imprint.

HL60 selectivity optimisation

To assess the CA15 imprint selectivity towards HL60, different parameters such as flowrate, the pre-treatment of the imprint with oxygen plasma, the bPEI and POL407 solution concentration were investigated. The aim was to improve the selectivity of the CA15 microbeads imprint towards the HL60 blood cancer cells and to allow the PBMCs to pass through the imprint. Oxygen plasma treatment was firstly found to positively impact cell selection with 38% selectivity observed after such treatment but only 25% selectivity with a non-treated imprint (ESI, Figure S4A). This is explained with the formation of additional negatively charged carboxyl groups ($-COO^-$) on the imprint surface after the oxygen plasma treatment which serve as better anchoring points of the cationic polyelectrolyte (bPEI).

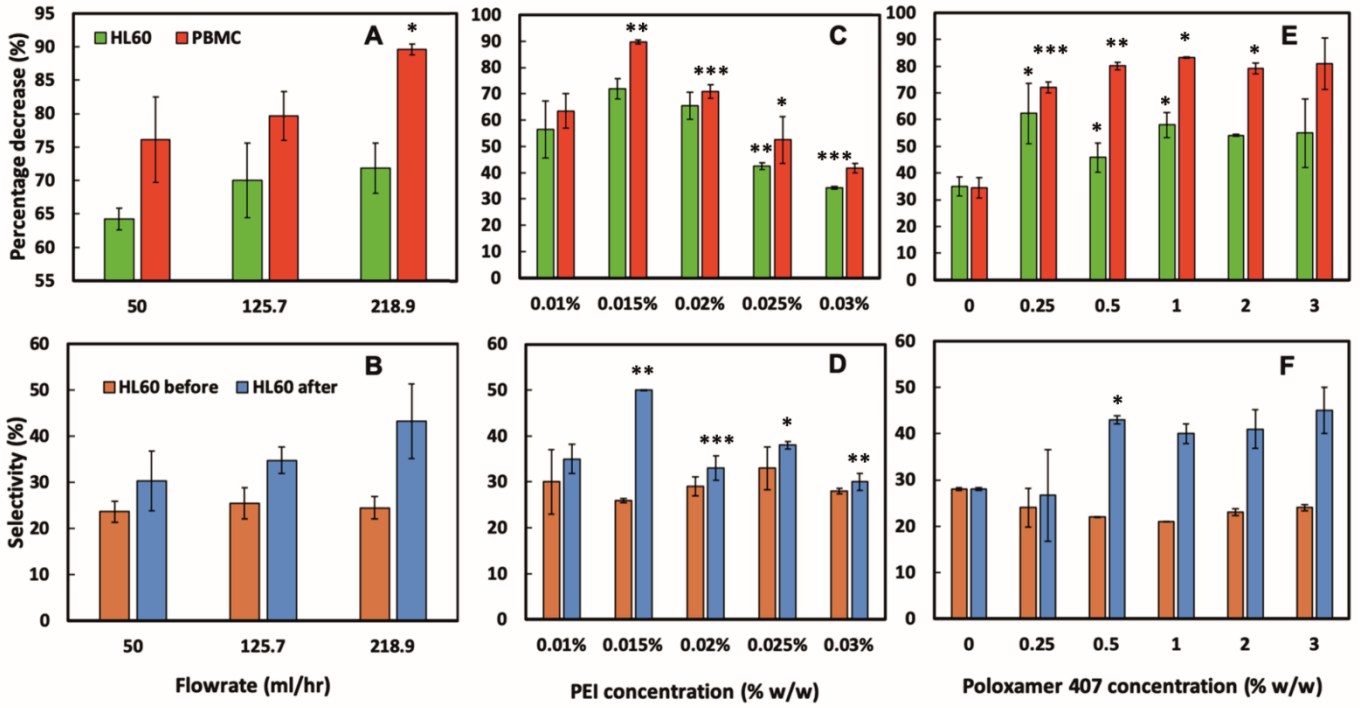

Figure 5. The influence on cell percentage decrease (due to cell capture) and cell selectivity of (A,B) Flow rate, (C,D) bPEI concentration on the imprint, and (E,F) POL407 concentration on the imprint after being passed through a 4cm oxygen plasma treated PMMA imprint with 0.015 wt% bPEI, at a flow rate of 218.9 mL/h. Data were expressed as average values ± standard deviations of the mean. P-values of less than 0.05 were considered significant. *P <0.05, **P <0.01, ***P <0.001. All Unpaired two-tailed t-tests were performed in GraphPad v7.0.4. Numeric data are given in Tables S2-S7 (ESI).

Therefore, all further experiments were carried out with oxygen plasma treated imprints. The length of the chip was then investigated and it was observed that imprints over 4 cm in length captured more cells proportionately, however at the expense of lower selectivity towards HL60 (Figure S4B, ESI). As it may be expected, the higher flowrate was associated with a lower retention of cells on the imprint. We found that the selectivity towards HL60 cells was optimal with a flowrate of 219 mL/hr at this treatment of the imprint. The particle imprint had an average selectivity of 43% in HL60 at 219 mL/hr after flushing but only 30% at a flowrate of 50 mL/hr. These results enabled us to select the flowrate of 219 ml/hr as the optimal for losing less HL60 and more PBMC from the imprint (Figure 5A,B). Different concentrations of bPEI (between 0.01 wt% and 0.03 wt%) were tested as per-treatment of the imprint in order to explore the effect of this cationic polymer on the HL60 cell selectivity of the imprint. This positively charged polymer adheres to the particle imprint and as a result increases the electrostatic interaction between the cells and the particle imprint surface. This effect is shown in terms of percentage of decrease of HL60 in Figure 5C: at 0.015 wt% bPEI treatment, 90% of the PBMCs were released from the imprint whereas at 0.03 wt% bPEI, only 40% were lost because they show higher affinity for binding with the positively charged imprint surface. In the terms of HL60 selectivity, 0.015 wt% bPEI treatment turned out to be the optimal concentration as evident from Figure 5D. In the others cases, the HL60 selectivity remains the same before and after flushing. In others cases, the selectivity remained the same before and after flushing. For optimisation of the concentration of the POL407 treatment of the imprint, different concentrations (between 0% and 3 wt%) of POL407 were used to evaluate the effect on the particle imprint in terms of cell capture and selectivity for HL60 (Figures 5E-F).

Selectivity for HL60 cells was achieved at POL407 concentrations above 0.5 wt%. The POL407 prevents very strong adhesions between the cells and the imprint and therefore improve the cell selectivity. Thus, predominantly cells that fit tightly into the imprint cavities will be retained as the interaction force of the cell with the imprint is proportional to the contact surface area. For PBMCs, which are much smaller than the imprint cavities, the contact area is very small (point contact) which makes them loosely bound and easy to flush out, which allows HL60 selectivity with respect to the PBMCs. At 0 wt% POL407 (no passivation), the particle imprint shows no selectivity between HL60 cells and the PBMCs: the percentage decrease is the same for both type of cells (35%) and the ratio between HL60 cells and PBMCs did not change (28%/72%) as evident from Figures 5E and 5F. This is explained with the indiscriminate strong attraction between the bPEI-treated imprint and the negatively charged cells. Above 0.25 wt% POL407 treatment, the particle imprint became selective for the HL60 cells. Our results show that above 0.5 wt% POL407, the particle imprint had been saturated with POL407 as the percentage decrease for the two types of cells and the selectivity were similar between 0.5 wt% and 3 wt%.

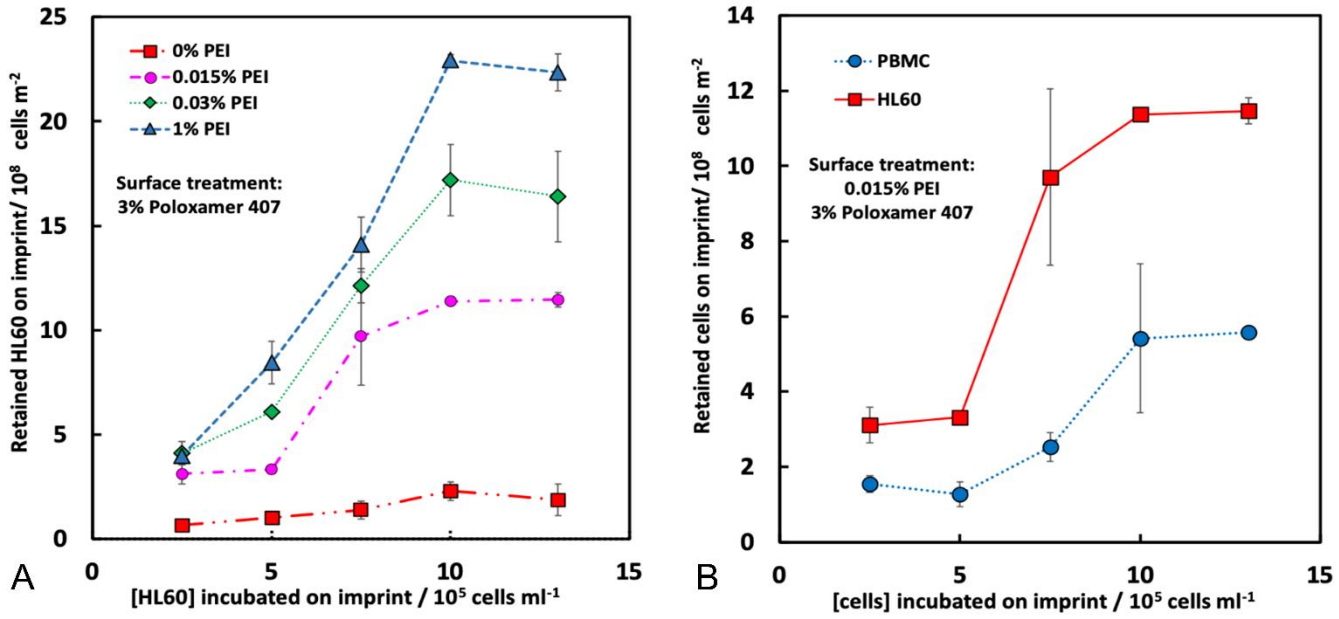

Figure 6. Cell retention on imprint as a factor of the cell seeding density and PEI concentration (A). Imprint used was 4 cm in length, coated with 3% POL407 and (B) preferential capture of HL60 against human PBMC on 4 cm PMMA microbeads imprint, oxygen plasma treated and coated with 0.015 wt% bPEI, 3 wt% POL407. The flushing flow rate was of 218.9 ml/h.

The particle imprint surface appeared to have become saturated with the highest cell concentration when pre-treated with 1% bPEI and 3% POL 407 (Figure 5). The cell retention was shown to be proportional to both the seeding cell ratio and the bPEI concentration. Higher bPEI concentrations, whilst retaining more HL60 to the imprint (Figure 6A) had the effect of loss of selectivity (Figure 5D) and therefore also increased PBMC retention. The optimal bPEI concentration was determined to be 0.015% (Figure 5C-D).

Finally, the cell retention of PBMCs and HL60 was determined (Figure 6B) with the optimised parameters. The proportion of retained cells was increased with increasing of the cell seeding concentrations for both cell types, however, this effect was far more pronounced for HL60 suggesting a specificity for HL60 over PBMCs was achieved (Figure 6B). We also conducted experiments with multiple seeding of the imprint up to four times on the chip to check the retention of HL60 cells on the imprint and its selectivity towards HL60 from HL60/PBMC mixture. According to Figure S7A (ESI), the percentage decrease of PBMC and HL60 follow a trend. These percentages decrease with the number of seeding up to a certain value. At this moment, the imprint becomes mostly saturated with HL60 cells. The percentage decrease at the 3rd and the 4th seeding are similar. This result can also be observed in Figure S7B, where the selectivity of the imprint for the HL60 cells was increasing until the 3rd seeding and then stagnates. The HL60 cell selection parameters were optimised to achieve blood tumour cell (HL60) specificity over healthy PBMCs. The experiments showed that the higher the flushing flowrate, the less amount of cells are retained on the imprint. However, it also indicated that the imprint becomes more selective with respect to HL60 cells when the flowrate is increased. The positively charged polyelectrolyte bPEI increases the electrostatic interaction between the cells and the imprint, hence the higher the concentration of the bPEI, the more the cells remain on the imprint. The passivating polymer, POL407 was used to weaken the cell adhesion and reduce non-specific binding of PBMCs therefore improving selectivity. Selectivity increased with increasing POL407 concentration up to a threshold of 0.5 wt%. Due to the smooth, spherical nature of the particles, relatively little asperity is observed with the CA15 particle imprint cavities as seen with cell imprints. Interactions dependent on the extracellular features are not seen with particle imprints and retention is dependent only on size matching between the targeted cells and the imprint. The optimal parameters for HL60 selective capture from the CA15 PMMA microbeads imprint were the following, flowrate: 219 mL/hr and imprint treatment with oxygen plasma, 0.015 wt% bPEI and 3 wt% POL407 from a ratio of 25%/75% between the HL60 cells and the PBMCs.

Particle imprints are cheaper and easier to mass produce than cell bioimprints which we have previously demonstrated to also be selective for circulating tumour cells.[29] The ease of production and functionalisation of particle imprints as described here, offer an advantage over bioimprinting however selectivity and retention rates were lower here suggesting a compromise between possible universal usage of a particle imprint versus increased selectivity and retention of a personalised bioimprint.

Particle imprints, however, have less surface targets compared to whole cell or molecule imprints where relatively small macromolecules such as polysaccharides, enzymes, aptamers, DNA sequences, antibodies as well as whole mammalian cells can also be targeted.[32-38] The methodology described here could be adapted for a range of purposes such as described here for capture but also for cell interrogation, for example response to drug treatments on an individualised basis. Depletion of blood cancer cells from healthy cells could result in improved outcomes for patients.[39]

Conclusions

Here we developed an alternative and inexpensive way to remove blood cancer cells from a mixture with peripheral blood mononuclear cells by using particle imprints. We identified microbeads of closely matching size distribution to the blood cancer cells. A layer of monodisperse CA15 PMMA microbeads of an average diameter of ~15 μm was produced and replicated on a large scale by PDMS and UV curable PU resin followed by copying of the produced master positive replica with Roll-to-Roll Nanoimprinting lithography to fabricate negative polymeric replicas of the original layer of microbeads. After suitable surface functionalisation of the imprint we carried out experiments with mixtures of HL60 (blood cancer cells) and healthy PBMCs to explore the selectivity of the imprint towards the blood cancer cells. The imprint was functionalised with oxygen plasma treatment, cationic polyelectrolyte and passivation with Poloxamer 407 polymer. Our method worked very well based on the large size difference between the HL60 and the PBMC. The HL60 cells closely fit in the imprint cavities and maximise their contact area with the imprint, while the PBMC have only a point contact and can be easily flushed out, leaving HL60 cell trapped on the imprint.

Conflicts of interest

There are no conflicts to declare.

Acknowledgements

PR acknowledges Ecole Nationale Supérieure de Chimie de Rennes for the opportunity to complete this work and the support from ERASMUS+ mobility grant. AAKD, DJA, LAM and VNP thank Cancer Research UK for the Pioneer Award funding and Higher Education Innovation Fund (UK) for supporting this work. JM also thanks University of Hull for supporting his PhD scholarship. We also thank Help for Health charity (Hull, UK) for supporting this research. The authors thanks Mr Tony Sinclair for the SEM images of the CA15 microbeads imprints.

ORCID

Anupam A. K. Das: 0000-0003-1948-8811
Jevan Medlock: 0000-0003-2425-3777
David J. Allsup: 0000-0001-6159-6109
Leigh A. Madden: 0000-0002-1503-1147
Dieter Nees: 0000-0001-9013-5651
Paul J. Weldrick 0000-0002-1791-5659
Vesselin N. Paunov: 0000-0001-6878-1681

References

1 J. Medlock, A.A.K. Das, L. A. Madden, D. J. Allsup, V. N. Paunov, *Chem. Soc. Rev.*, 2017, **46**, 5110–5127
2 K. Ren, R.N. Zare, *ACS Nano*, 2012, **6**, 4314–4318
3 A.L. Bole and P. Manesiotis, *Adv. Mater.*, 2016, **28**, 5349–5366.
4 Y. Ge and A.P. Turner, *Trends Biotechnol.*, 2008, **26**, 218–224.
5 G. Vasapollo, R. Del Sole, L. Mergola, M.R. Lazzoi, A. Scardino, S. Scorrano and G. Mele, *Int. J. Mol. Sci.*, 2011, **12**, 5908–5945.
6 F.L. Dickert and O. Hayden, *Analyt. Chem.*, 2002, **74**, 1302–1306.
7 O. Hayden, K.J. Mann, S. Krassnig, F.L. Dickert, *Angew. Chem. Int. Ed. Engl.*, 2006, **45**, 2626–2629.
8 A. Mujahid and F.L. Dickert, *Sensors*, 2015, **16,** 51.1–17.
9 Z. Zhang, J. Li. L. Fu, D. Liu, L. Chen, *J. Mater. Chem. A*, 2015, **3**, 7437-7444.
10 M. Jia, Z. Zhang, J. Li, X. Ma, L. Chen, X. Yang, *Trends Anal Chem,* 2018, **106**, 190-201.
11 Z.Altinas, M. Gittens, A. Guerreio, K-A Thompson, J. Walker, S. Piletsky, I.E. Tothill *Anal. Chem.*, 2015, **87**, 6801-6807
12 L. Chen, S. Xu, J. Li, *Chem. Soc. Rev.* 2011, **40**, 2922-2942
13 C. O'Brien, E. S. Prideaux and T. Chevassut, *Adv. Hematol.*, 2014, **2014**, 103175.1-15.
14 E. Estey and H. Döhner, *The Lancet*, 2006, **368**, 1894–1907.
15 J.L. Shipley and J.N. Butera, *Exp. Hematol.*, 2009, **37**, 649–658.
16 Y. Ofran, M.S. Tallman and J.M. Rowe, *Blood*, 2016, **128**, 488–96.
17 D.A. Pollyea, H.E. Kohrt and B.C. Medeiros, *Brit. J. Haematol.*, 2011, **152**, 524–542.
18 J.E. Kolitz, *Brit. J. Haematol.*, 2006, **134**, 555–572.
19 J.M. Bennett, D. Catovsky M-.T. Daniel, G. Flandrin, D.A.G. Galton, H.R. Gralnick and C. Sultan, *Brit., J. Haematol.*, 1976, **33**, 451–458.
20 A.K. Burnett, *Hematol. Amer. Soc. Hematol. Educ. Program,* 2012, **2012**, 1–6.
21 C.S. Viele, *Semin. Oncol. Nurs.*, 2003, **19**, 98–108
22 H. Dombret and C. Gardin, *Blood*, 2016, **127**, 53–61
23 C.S. Hourigan and J.E. Karp, *Nat. Rev. Clin. Oncol.*, 2013, **10**, 460–471.
24 F. Ravandi, R.B. Walter and S.D. Freeman, *Blood Adv.*, **2**, 2018, 1356–1366
25 R. Fakhrullin, I. Choi, Y. Lvov, *Cell Surface Engineering: Fabrication of Functional Nanoshells*, Cambridge: Royal Society of Chemistry, 2014, pp. 164.
26 J. Pan, W. Chen, Y. Mab, G. Pan, *Chem. Soc. Rev.*, 2018, **47**, 5574–5587
27 L, Chen, X. Wang, W. Lu, X. Wu, J. Li, *Chem. Soc. Rev.*, 2016, **45**, 2137–2211
28 E. Estey and H. Döhner, *The Lancet*, 2006, **368**, 1894–1907.
29 A. A. K Das, J. Medlock, H. Liang, D. Nees, D. Allsup, L.A. Madden, V.N. Paunov, *J. Mater. Chem. B*, 2019,**7**, 3497-3504

30 M. Leitgeb, D. Nees, S. Ruttloff, U. Palfinger, J. Götz, R. Liska, M. R. Belegratis, B. Stadlober, *ACS Nano*, 2016, **10**, 4926–4941
31 H. Döhner, E.H. Estey, S. Amadori, F.R. Appelbaum, T. Büchner, A.K. Burnett, H. Dombret, P. Fenaux, D. Grimwade, R.A. Larson, F. LoCoco, T. Naoe, D. Niederwieser, G.J. Ossenkoppele, M. A. Sanz, J. Sierra, M. S. Tallman, B. Löwenberg and C. D. Bloomfield, *Blood* 2010 **115**:453-474.
32 A.L. Bole and P. Manesiotis, *Adv. Mater*., 2016, **28**, 5349–5366.
33 T.S. Bedwell and M.J. Whitcombe, *Anal. Bioanal. Chem.*, 2016, **408**, 1735–1751.
34 S. Sacanna, W.T.M. Irvine, P.M. Chaikin and D.J. Pine, *Nature*, 2010, **464**, 575–578.
35 J. Borovicka, S.D. Stoyanov, V.N. Paunov, *Nanoscale*, 2013, **57**, 8560–8568.
36 J. Borovicka, W.J. Metheringham, L.A. Madden, C.D. Walton, S.D. Stoyanov, V.N. Paunov, *J. Am. Chem. Soc*., 2013, **135**, 5282–5285.
37 J. Borovicka, S.D. Stoyanov, S.D., V.N. Paunov, *MRS Proceedings*, 2012, 1498, mrsf12-1498-l10-06, doi:10.1557/opl.2013.14.
38 J. Borovicka, S.D. Stoyanov, V.N. Paunov, *Phys. Rev. E*., 2015, **92**, 032730.
39 C.S. Hourigan and J.E. Karp, *Nat. Rev. Clin. Oncol*., 2013, **10**, 460-471.
40 O.J. Cayre, V.N. Paunov, *J. Mater. Chem*., 2004, **14**, 3300-3302.

